JOURNAL OF AIRCRAFT
Vol. 32, No. 5, September–October 1995

Analysis of Rolled Delta Wing Flows Using Effective Sweep and Attack Angles

Eric J. Stephen*
Frank J. Seiler Research Laboratory, U.S. Air Force Academy, Colorado 80840-6272

Flow visualization data over the suction surface of a 65-deg swept delta wing were recorded at a 30-deg incidence angle for a range of static roll angles (−42 to 42 deg) and Reynolds number of 9.0 × 10^5. The data were reduced to provide information on the vortex relative position and the burst point location. The results were compared to previously recorded rolling moment data, to provide an understanding of the relationship between flow behavior and aerodynamic loading. The combination of roll about the body axis and an axis incidence angle with the flow induced a sideslip angle relative to the wing. Combining the sideslip angle with the nominal leading-edge sweep of the wing provided an effective leading-edge sweep angle. Using the effective sweep angle, along with the previous data for unyawed delta wings, the flow behavior over either side of the wing was predicted. Extending this analysis suggested the presence of nonzero trim positions in roll, based on wing movement in and out of a stalled regime. These trim positions have been recorded in free-to-roll experiments.

Nomenclature

s = local semispan
x = chordwise position
y = spanwise position
z = position normal to the wing surface
α = angle of attack between the wing and the freestream
Δ = increment
Λ = sweep angle
σ = incidence angle between the root chord and the wind-tunnel floor
ϕ = roll angle about the body axis subscripts

Subscripts
bp = burst point
eff = effective
0 = nominal

Introduction

THE flow over the delta wing planform has been of interest since the 1950s due to the delta wing design used on high-speed aircraft. The delta wing provides a unique type of flowfield with the formation of large helical vortices over the upper wing surface. This flow structure allows the delta wing to maintain lift to high angles of attack when compared to the conventional straight wing.

With the current emphasis on improving aircraft maneuverability, the flight envelope is being pushed to higher limits, even into the poststall regime. In these flight regimes the stall characteristics of the wing become important. For the delta wing, a precursor to stall on the delta wing[1] is the movement of the burst point to a position over the wing. Therefore, the position of the vortex burst point can be an indicator for wing performance.

To evaluate the fluid dynamics and aerodynamic loading of the delta wing undergoing high-angle-of-attack maneuvers, the Canadian National Research Council (NRC) developed a comprehensive test program for testing a 65-deg swept delta wing in a wind tunnel.[2] Force balance, surface pressure, and flow visualization data were recorded for the flow over a delta wing, which was held at an incidence angle of 30 deg and was forced statically and dynamically through a range of roll angles about the body axis.

The force balance results have been discussed previously.[2] In this article the flow visualization will be discussed with emphasis on the behavior of the burst point and the changing structure of the vortex flow for different geometric orientations. This presentation is limited to the static results. The results were analyzed according to the effective sweep angles on leading edges of the wing. The effective sweep angle was determined by the relative orientation of the leading edge to the freestream. This analysis provides some physical interpretation of the rolling moment results that have been previously published.

Methods

The delta wing model and the tunnel setup have been documented by Hanff[2] (Fig. 1). The model was a 65-deg swept-back flat plate model with a 25-deg knife-edge bevel and the root chord length was 24.48 in. The root chord axis of the model was held at a 30-deg incidence angle relative to the floor of the wind tunnel. Roll angles were measured about this axis. Kerosene smoke was injected forward of the apex and was entrained into the two vortices of the suction surface of the wing. A movable set of optics was designed to produce

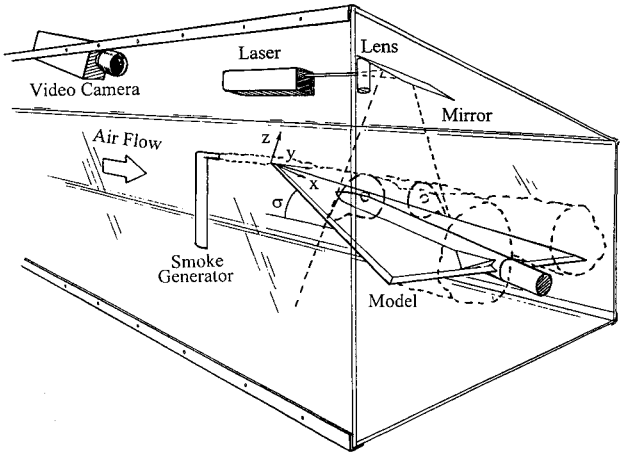

Fig. 1 Caricature of the experimental setup.

Received May 9, 1994; revision received Feb. 18, 1995; accepted for publication Feb. 20, 1995. This paper is declared a work of the U.S. Government and is not subject to copyright protection in the United States.

*Research Associate, 2354 Vandenberg Drive, Suite 6H79. Member AIAA.

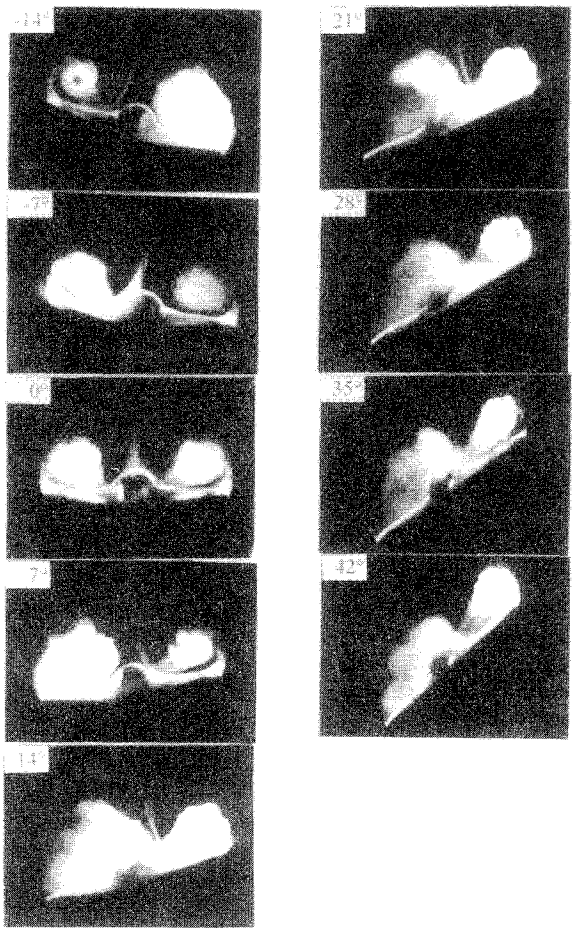

Fig. 2 Flow visualization images, recorded at the 60% chord position, σ = 30 deg, ϕ = −14 to 42 deg.

a laser sheet normal to the root chord axis. The laser sheet was moved along the model from the trailing edge to the apex illuminating cross-sectional cuts of the conical vortices.

The flow visualization was reduced using an image analysis program documented by McLaughlin.[3] The image analysis program first identified the wing and its roll orientation. Then the position and size of both leading-edge vortices, as well as the burst condition, were determined for each analyzed frame of the video data. Vortex size was determined by the area of the smoke illuminated over either side of the wing. The vortex position was initially estimated as the centroid of that illuminated smoke region.

The burst condition of the vortex was determined by the presence or absence of coherent core flow, denoted by a small darkened circle near the center of the illuminated smoke region (Fig. 2, frame a). Reasons for the dark appearance of the core flow are discussed in Ref. 4. If the core was detected, the core center was used to estimate the position of the vortex.

Other researchers have discussed the nature of vortex burst,[5–8] either as the sudden expansion of the core (bubble breakdown) or as a sudden core trajectory change from a line to a helix (helical breakdown). In either case the breakdown was manifested in the flow visualization as the expansion of the darkened core, followed by its disappearance as the core flow diffuses. Once the general spatial region of core diffusion was determined from the image analysis program, the region was reviewed manually to determine where core expansion initiated. The burst location was recorded as the chordwise position where the darkened core began to expand. A similar burst identification criteria was used previously by Kegelman.[9] Since the burst location is not fixed, this technique determined the most upstream burst location.

Results

Examples of the flow visualization data (viewed from the front[2]) are shown in Fig. 2 for roll angles from −14 to 42 deg. These results were recorded for the 60% chord position. Since the vortex remains conical over the surface, the relative spanwise position of the vortex (y/s) was nearly constant, and so a single position was representative of the vortex flow position over the whole wing. The frames show the smoke, entrained in the vortices on either side of the rolled wing and illuminated by a laser sheet perpendicular to the roll axis. The wing can be seen highly illuminated at the bottom of each frame. The hump in the center of the wing is the housing for the force balance and mounting apparatus.

The images show that flow over the leeward (upper) side produced a more compact vortex with a more aft burst location. The aft burst location was indicated by the presence of a core in the leeward vortex only. At the higher roll angles the core on the leeward side was present, but was washed out by the high intensity of the illuminated smoke. The leeward vortices also exhibited vortical ornamentation, evidenced by the wavy outline of the illuminated smoke. The ornamentation is the discretization of the outer shear layer into a series of vortices similar to that shown by Gad-el-Hak[10] (Fig. 2, second column).

For roll angles greater than 7 deg, the flow on the windward wing no longer exhibited the organized outboard flow along the surface, indicative of a vortex. This flow was appropriately referred to as separated rather than as vortical flow. Huyer[11] referred to this type of flow as "globally separated" for a delta wing with no sideslip, Cornelius[12] uses the term "ultimate burst." As the roll angle increased past 14 deg, the smoke on the windward side did not fill the separated region completely, but remained in the inboard part of the region. The height of the separated region could still be estimated, however. From the estimation the separation height reached a maximum at 21-deg roll, declining with higher angles.

The trend of having a small, coherent vortex on the leeward side and a burst vortex or separated flow on the windward side was consistent in all the frames. The negative roll angles were included in Fig. 2 to show the symmetry of the tests. The lack of antisymmetry between the flowfields for 14 and −14 deg suggests that the roll angles may have had a slight offset in the zero roll position, possibly because of support interference.[13]

From the flow visualization data the vortex positions, as well as the vortex burst point locations, were tracked. The relative spanwise positions of the vortex y/s at the 60% chord position are shown in Fig. 3 for the range of roll angles from −42 to 42 deg. As discussed previously, these data represent the spanwise core positions when a vortex core was apparent. When a vortex core was not apparent, i.e., the vortex was

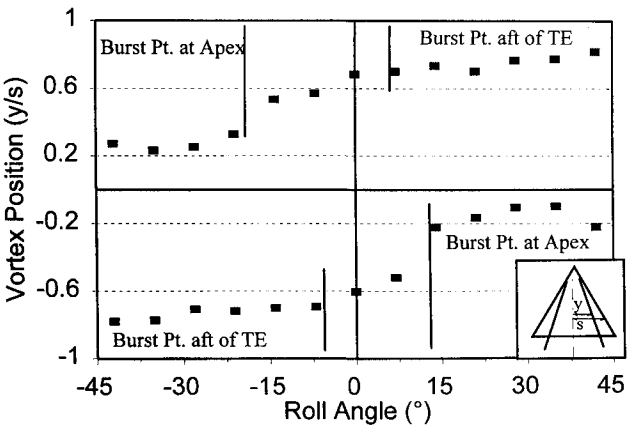

Fig. 3 Vortex relative spanwise positions, recorded at the 60% chord position, σ = 30 deg, ϕ = −42 to 42 deg.

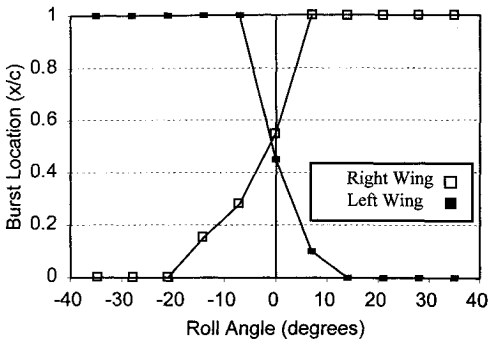

Fig. 4 Vortex burst point relative chordwise positions; σ = 30, ϕ = −42 to 42 deg.

burst or the flow was separated, the data were the spanwise centroid positions of the illuminated smoke. The spanwise position is shown because the far inboard spanwise position corresponded with separation of the flow. Therefore, these data provide an indication of the changing structure of the flow.

The data on the upper half of the graph correspond to the right wing shown in Fig. 3, while the lower half data correspond to the left wing. The general trend of the vortex position was to move inboard as the wing moved into a more windward position. The vortices reached a most inboard position near 35- and −35-deg roll for the left and right wings, respectively. A lack of antisymmetry was apparent at ϕ = 0 deg, with the vortex on the left moving slightly further inboard. This may also be a result of support interference[13] as suggested earlier.

Several regions have been labeled on the graph to show the relation between vortex position and burst condition. When the burst point was aft of the trailing edge or over the surface, there is a near-linear relationship between the roll angle and vortex position. When the burst point reached the apex, the character of the flow changed from vortex to separated flow. Also, the smoke did not reach the outboard separated region, as was described. Both of these factors contributed to the inboard movement of the position data.

The burst point data for either wing are shown in Fig. 4 with the relative chordwise burst location plotted vs roll angle. Similar to the position data, these data show the inverse behavior of the burst point data from one wing to the other. As the roll angle increased, the burst point on the right wing moved aft while the burst point moved forward on the left wing. The intersection of the two curves occurred at a slightly negative roll angle.

The graph shows that the burst point was only over the surface for a small portion of the test range. When the burst point was at or aft of the trailing edge, the data show the burst point at the trailing edge. Since the laser sheet did not move past the end of the model, it was not possible to track the burst point aft of the wing. The data show the burst point at the apex for all cases where no vortex core was apparent over the wing.

Discussion

In order to discuss these results, a conceptual model for delta wing flow is suggested. For the model, it is postulated that the organization of vortices over the delta wing is a function of the sweepback angle, the angle of attack, and the influence of the vortex on the opposite side of the wing. The sweep angle and the angle of attack determine the orientation of the leading edge relative to the flow. The orientation should determine the vorticity flux from the leading edge into the delta wing vortex. The sweep angle and the angle of attack also determine the region shadowed from the freestream in which vorticity can accumulate. The sweep angle and angle of attack are important parameters in the determination of vortex organization.

The influence of the opposite vortex, for delta wings with sweep angle less than 70 deg, would be to impose a downward velocity component on the vortex. At higher sweep angles the vortex–vortex interactions become more complicated. The magnitude of the influence is determined by the strength and the proximity of the two vortices. Roos and Kegelman[14] have shown that the spanwise position of the vortex core is roughly 60% of the semispan from the root chord, a function of the sweep angle. For a lower swept wing the vortices are farther apart. Nelson[4] has shown that the circulation contained in the vortex is also proportional to the sweep angle. The lower swept wing produces higher circulation values. Since these two effects act counter to one another, as a first approximation for analysis, the influence of the opposite vortex is assumed to be constant. Changes in vortex development are therefore assumed to be only a function of the sweep angle and angle of attack. This appears to be true from the half-models results reported by Roos,[14] which showed excellent flow similarity to full delta wing models with sweep angles of 60 and 70 deg. This similarity of flowfields for half models does not indicate that aerodynamic loading is the same as a full delta wing because of vortex wall interactions.

The implication for a yawed delta wing is that the flow will develop according to the effective sweep of the wing leading edge. The effective sweep would be a combination of the nominal sweep of the wing and the sideslip angle. The flow over the windward wing would develop as if the sweep angle were reduced and vice versa for the leeward wing. The trend for this behavior was seen in previously reported burst point data[15] over yawed delta wings. The burst point on the windward wing moved forward with an increase in yaw, consistent with a decrease in the leading-edge sweep angle.

In the current tests, the incorporation of roll onto the delta wing at an angle of attack induced a sideslip angle while reducing the angle of attack. Equations for calculating the reduced angle of attack and the sideslip angle as functions of ϕ and σ are found in Ericsson[16]:

$$\alpha(\phi) = \tan^{-1}(\tan\sigma\cos\phi)$$

$$\Delta\Lambda(\phi) = \tan^{-1}(\tan\sigma\sin\phi)$$

The effective sweep angle of the leading edge would be determined by a combination increment of the sweep angle due to the induced sideslip angle and the nominal sweep angle Λ:

$$\text{windward wing: } \Lambda_{\text{eff}} = \Lambda_0 - \Delta\Lambda$$

$$\text{leeward wing: } \Lambda_{\text{eff}} = \Lambda_0 + \Delta\Lambda$$

Using the calculated effective sweep angle and angle of attack, combined with previously reported burst point data, the burst point locations for the rolling delta wing could be predicted.

In order to address the accuracy of this simple estimation technique, burst data were taken from several sources[9,14,17–20] for a range of sweep angles and angles of attack. These data are plotted in Fig. 5. These data were collected over as wide a range of sweep angles as possible. On the low end, researchers have reported no evidence of a coherent vortex over the surface for a sweep angle of 45 deg or less, regardless of angle of attack. The upper end is obviously limited to less than 90 deg. The angle-of-attack range was determined by the presence of the burst point over the surface. For any model the burst point was over the surface for 10–15-deg angle-of-attack range. For the 85-deg delta wing the burst point would reach the apex at about 70-deg angle of attack.

The different symbols on the graph represent the different sweep angles. The separation of the symbols shows a shift to higher angles of attack with increased sweep angle. The scatter

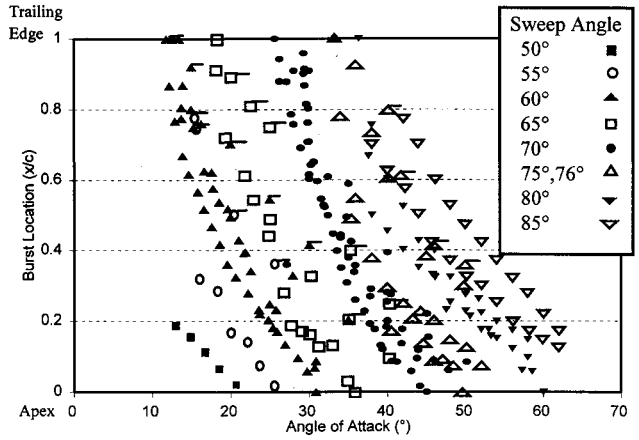

Fig. 5 Relative vortex burst positions vs angle of attack for Λ = 50–85 deg (Refs. 9, 14, 17–20).

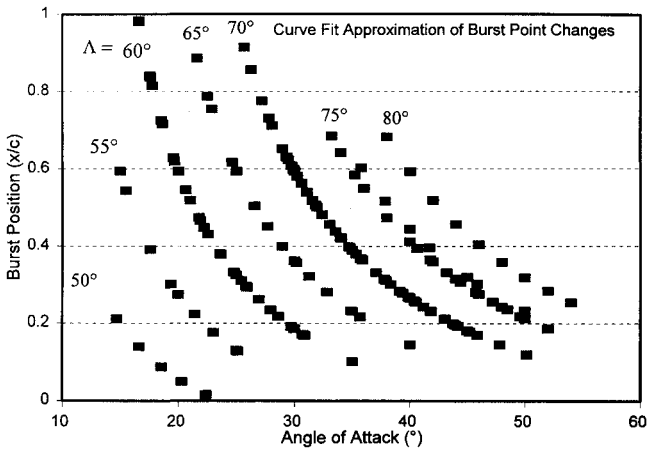

Fig. 6 Approximated burst point data based on a curve fit of the data in Fig. 5.

in the data was due to differences in the model shape. Kegelman[9] has shown that this scatter can be reduced by comparing wings with the same leading-edge shape. The flagged data points were taken from Wentz.[18] Their test model had a flat surface and a convex surface. Data taken using the convex surface as the upper surface produced a definite change in the burst behavior. Therefore, the data from the convex-up tests are flagged. All other data were taken with flat plate models.

Visual inspection of the data indicated that the burst-point location had a similar function of the angle of attack, regardless of the sweep angle. Lambourne[21] had previously shown that the burst-point location data, under different sweep conditions, collapsed on a single curve when plotted against $\cos^{-1}(\cos\alpha \sin\Lambda)$. Plotting the collection data from Fig. 5 against this function did not produce the same level of collapse that Lambourne had reported, and so another function was developed using curve-fitting techniques:

$$x_{bp} = \left[\frac{0.00741\Lambda - 0.287}{\alpha - (0.00866\Lambda - 0.3573)}\right] - 0.25$$

It is stressed that the model is not based on a physics of the flowfield. Rather, a function for the burst-point location was sought to model sweep and attack angle effects in order to compare the nominal behavior of the flow over delta wings to that under yawed conditions. The results of applying this function to the Λ and α conditions for Fig. 5 are shown in Fig. 6.

The burst-point function was applied to the data taken from McKernan[15] in Fig. 7. The burst-point location data were recorded for a 70-deg swept wing over a range of angles of attack and sideslip angles. The data were presented for the windward side of the wing only. The burst-point location was estimated by substituting Λ_{eff} in the burst-point function. The results show excellent agreement between the predicted vortex burst position and the measured values, suggesting that, at least in this limited range, the flowfield on either side of the delta wing can be determined by the effective sweep angles and angle of attack.

The same function was applied to the current data for a delta wing with a combination of pitch and roll. The comparison between the measured data and that predicted by the function are shown in Fig. 8. For this comparison the data from Fig. 4 were replotted vs the effective sweep angle of each side of the wing. For these cases, the burst-point function predicted the experimental data within 20% chord for effective sweep angles below 70 deg. A 20% chord change in the burst location with different leading-edge shapes was not unreasonable, since most of the reference data were collected on models with flat upper surfaces, and the upper surface of

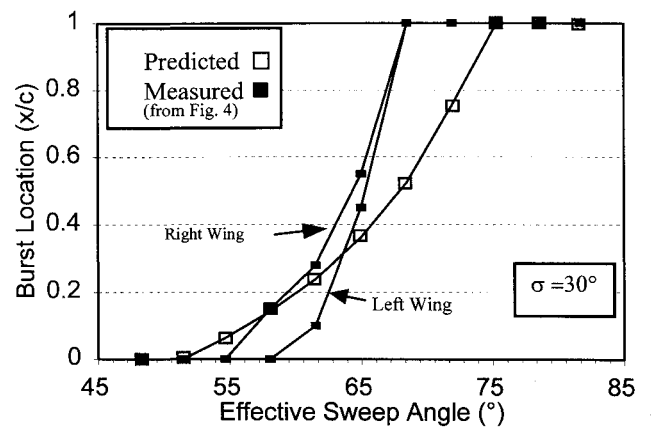

Fig. 7 Burst point position data taken on a yawed 70-deg swept delta wing compared to the curve-fit approximation.[15]

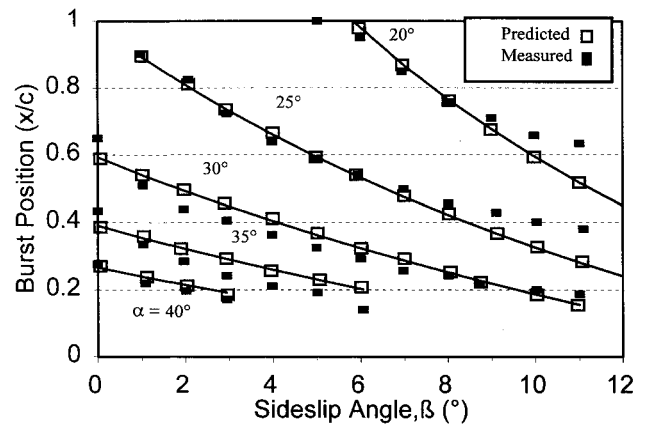

Fig. 8 Burst point position data taken on the 65-deg delta wing model compared to the curve-fit approximation.

this delta wing model was beveled at the edges.[22] Also, it was difficult to determine burst locations forward of 20% chord because the bright illumination of the dense smoke in that region washed out the small, dark core flow. It is noted that the excellent comparison with McKernan's data, for the windward wing only, was also for effective sweep angles less than 70 deg.

These results show that a burst-point equation based on the nominal wing configurations provided accurate burst-point estimates for effective sweep angles less than 70 deg. Above 70 deg the trend was predicted, but the error increases. This

may be indicative of the scatter in the data on which the predictive equation was based or it may indicate a breakdown in the premise of opposite vortex influence at higher sweep angles.

The first possibility could be resolved with a parametric set of flow visualization tests over delta wings with common leading-edge shapes and a wide range of sweepback angles. As for the second possibility, it has been shown that the vortex sheets separating from both sides of the wing come in contact prior to vortex breakdown[18] for sweep angles greater than 75 deg. For angles of attack above initial vortex sheet contact, the vortex cores can be forcibly displaced off the surface. This is presumably an effect of the interaction between the vortices due to their proximity. This core displacement may explain stall for higher sweep angles prior to the burst point reaching the apex.[18] For the case of the yawed wing, with lower nominal sweep than the effective value, opposite vortices would not have the same proximity and would not interact in the same manner. This may be why this predictive technique becomes less accurate for effective sweep angles greater than 70 deg.

This flowfield dependence on the effective sweep and attack angles was used to estimate the burst-point behavior. The roll angle range, within which the burst point was over the surface, was only a small portion of the tested roll angle range. In the remainder of the range this effective sweep angle concept allows for speculation about the static loading behavior. In particular, trends in the rolling moment data could be estimated.

Using the effective angle estimates discussed earlier, the effective leading-edge sweep and attack angles were calculated for a 65-deg swept wing with a 30-deg nominal angle of attack and a range of roll angles. The results are plotted as the solid curve in Fig. 9. The upper half of the curve represents the leeward wing and the lower half, the windward wing.

Also included on the graph (open circles) are the stall angles for a range of delta wing sweep angles.[1,11,17,18] These data were taken from the flow over complete delta wing models. The flat plate rectangular wing was assumed to stall at about 7-deg angle of attack. The dashed line on the graph represents an average stall angle for the different sweep angles and divides the graph into stalled and unstalled regions. The effective sweep-angle analysis would predict that movement of the windward wing into the stalled region would cause the flow over that wing to stall, along with a loss of lift.

Finally, a line was included at the 90-deg effective sweep position and is denoted as wingtip. Erickson[23] has shown, on highly swept wings, imparting a sideslip angle to the wing can cause the vortex to move off of the surface. The 90-deg position provided a limit for this type of behavior.

The results on Fig. 9 can be related to the rolling moments in the following manner. Earnshaw[24] showed that the lift curve slope for a lower swept wing is higher than for a higher swept wing if neither has stalled. On the figure the windward wing, with the lower effective sweep angle, would produce more lift than the leeward wing at the same angle of attack. If the moment arms about the root chord are assumed to be nearly equal, this loading behavior would provide a stabilizing rolling moment and a trim position at 0 deg of roll.

Movement of the windward wing into the stalled region would cause the lift produced by the windward wing to decrease. The leeward lift could then dominate and produce an unstable rolling moment. A limit factor to instability could be the movement of the leeward wing past the 90-deg effective sweep angle, which would cause the vortex to move off the surface, reducing the lift due to the presence of the vortex. The result would be an increase in the correcting moment back to 0 deg roll. Similarly, movement of the windward wing back into the unstalled region at high roll angles should again produce a correcting moment back toward 0 deg.

For the test data (Λ = 65 deg, σ = 30 deg) the effective angle curve is in the unstalled region at 0-deg roll. As described previously, a statically stable roll point would be expected at 0 deg. This point was demonstrated in free-to-roll tests reported by Hanff.[2]

The effective angle curve intersects the estimated stall curve at approximately 10-deg roll. If the effective angle analysis holds, a destabilizing rolling moment would be produced for higher roll angles. When the roll angle was increased to 50 deg, however, the windward wing returns to the unstalled region and a stabilizing rolling moment would again be produced. A zero rolling moment and nonzero stable roll position must then occur somewhere between 10–50 deg of roll. Rolling moment and free-to-roll data for a 65-deg delta wing, reported by Hanff,[2] showed this general trend in the moment data with nonzero, static stability (critical) points at ±21 deg.

Further results, also for the 65-deg model, were reported by Hanff[24] for attack angles of 20, 25, 35, and 40 deg. The corresponding stability points were at 0, |1.5|, |11|, and 0 deg, respectively. Using the current analysis, effective angle diagrams were plotted for these cases in Figs. 10–13.

In Fig. 10 the entire effective angle curve was well out of the stalled region for all cases. Only a stability point at 0 deg would be expected for this case, consistent with the Hanff's experimental results. The same results would be expected from Fig. 11. Hanff reported a slight deviation from that point.

For an attack angle of 35 deg (Fig. 12), the 0-deg roll position on the curve has moved into the stalled region. No

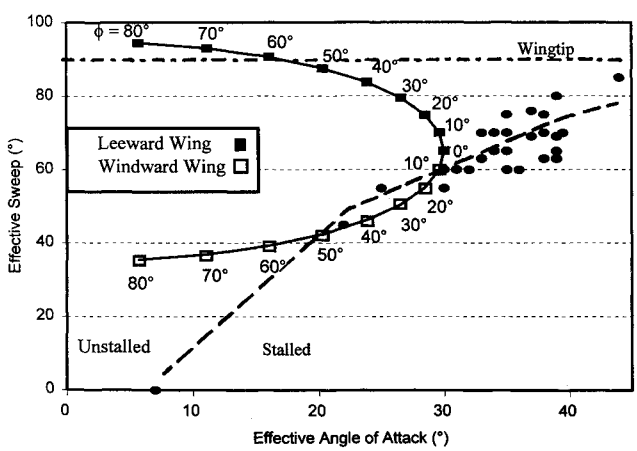

Fig. 9 Effective sweep angle and effective angle-of-attack curve plotted over the effective angle map showing the stalled regime for the delta wing; σ = 30 deg, Λ = 65 deg, ϕ = 0–80 deg.

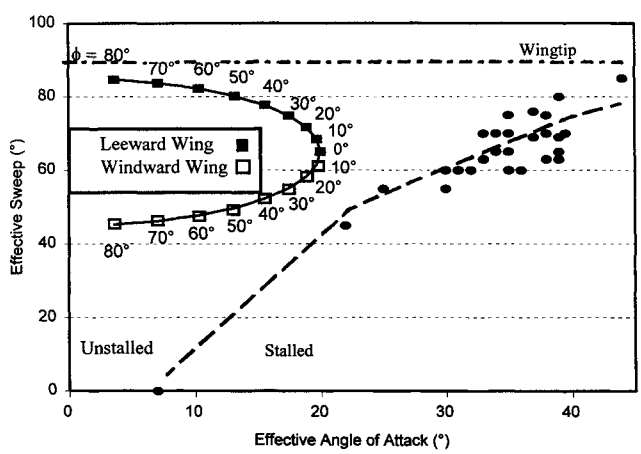

Fig. 10 Effective sweep angle and effective angle-of-attack curve plotted over the effective angle map showing the stalled regime for the delta wing; σ = 20 deg, Λ = 65 deg, ϕ = 0–80 deg.

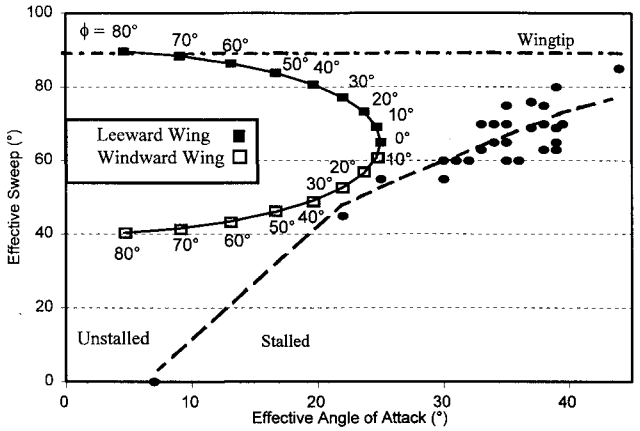

Fig. 11 Effective sweep angle and effective angle-of-attack curve plotted over the effective angle map showing the stalled regime for the delta wing; σ = 25 deg, Λ = 65 deg, ϕ = 0–80 deg.

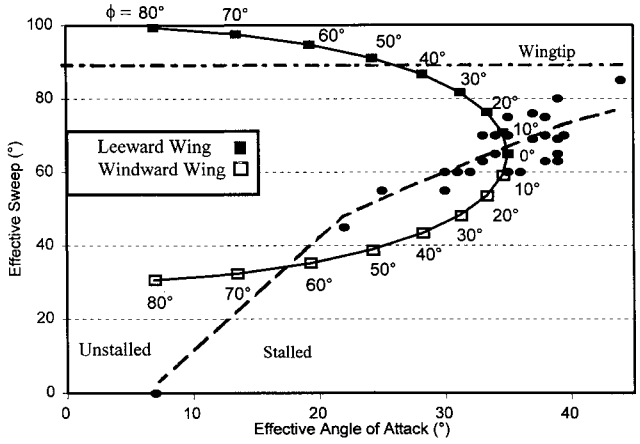

Fig. 12 Effective sweep angle and effective angle-of-attack curve plotted over the effective angle map showing the stalled regime for the delta wing; σ = 35 deg, Λ = 65 deg, ϕ = 0–80 deg.

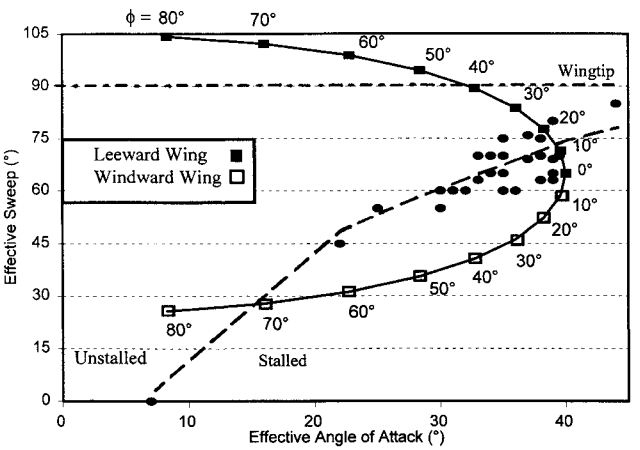

Fig. 13 Effective sweep angle and effective angle-of-attack curve plotted over the effective angle map showing the stalled regime for the delta wing; σ = 40 deg, Λ = 65 deg, ϕ = 0–80 deg.

rolling moment would be expected under these symmetric conditions, however, an increase in the roll angle moves the leeward wing into the unstalled region producing a destabilizing moment. No zero stability point was expected for this case. This analysis would again suggest the presence of a nonzero stability point. It does not provide the |11 deg| trim point value reported by Hanff[24] and again by Jenkins.[25] This analysis, at first, might suggest that the stability point would be at a position greater than the 21-deg value reported for an attack angle of 30 deg since the return to the unstalled region occurs at a higher roll angle. Other considerations, however, would have to be the roll angle where the leeward wing passes 90-deg effective sweep and that the wing is stalled for 0-deg roll. Also, the flow behavior on either side of the wing, once one side has stalled, can no longer be considered as independent. These factors make it more impossible to predict where the trim point would be located using this simple analysis.

In Fig. 13 (α = 40 deg) the wing is well into the stalled region for ϕ = 0 deg. In this case, the 0-deg roll position may become neutrally stable. Again, it would be difficult to make accurate estimates of any nonzero statically stable roll positions.

Increasing the wing sweep angle could move the effective angle curve up and out of the stalled region. Rolling moment data from free-to-roll tests by Thompson[26] for an 80-deg sweep wing shows no signs of the nonzero trim points. Increasing the sweep angle, however, moves the models into a regime where wing rock can occur, a dynamic problem that will not be addressed here.

For sweep angles less than 70 deg, the model predicts three stable point cases; one, two, or three stable roll positions. One point can occur at 0-deg roll when the effective angle curve is outside the stall region. Two statically stable points can occur when the 0-deg point is slightly in the stalled region. Three points can occur when the 0-deg roll position is slightly outside the stalled region and the effective angle curve passes through the stalled region.

Conclusions

The results show that the vortex behavior on either side of a delta wing can be related to the effective sweep and the attack angles of the leading edge. Applications of an empirical equation for the burst point based on unyawed data showed good comparisons to yawed data for effective sweep angles below 70 deg. The differences may be due to the influence of the vortex on the opposite wing. This issue could be addressed in a parametric study comparing the flow over yawed and unyawed wings. Comparison of existing data from several authors is difficult due to the sensitivity of the flow to model leading-edge shape.

The empirical equation was not based on physical phenomenon, but rather was a curve fit for comparison between yawed and unyawed data. A similar formula based on the fluid dynamic should be developed. Such an equation could then be extended to apply to the dynamic data for which the reported data was a baseline. The importance of the effective sweep and attack angles, shown here, may help to develop this equation.

Finally the nonzero stability points, shown by Hanff, have been discussed from a different point of view. The simple analysis using effective sweep and attack angles provides an explanation for the general trends. An extended study to try to define the sweep and attack angle limitations of this behavior and to predict these points would be valuable.

References

[1]Lee, M., and Ho, C.-M., "Vortex Dynamics of Delta Wings," *Frontiers in Experimental Fluid Mechanics, Lecture Notes in Engineering*, Vol. 46, Springer–Verlag, Berlin, 1989, pp. 365–427.

[2]Hanff, E. S., and Jenkins, S. B., "Large-Amplitude High-Rate Roll Experiments on a Delta and Double Delta Wing," AIAA Paper 90-0224, Jan. 1990.

[3]McLaughlin, T. E., "Aerodynamic Foundation for Use of Unsteady Aerodynamic Effects in Flight Control," Ph.D. Dissertation, Univ. of Colorado, Boulder, CO, Aug. 1992, pp. 121–132.

[4]Nelson, R. C., and Visser, K. D., "Breaking Down the Delta Wing Vortex: The Role of Vorticity in the Breakdown Process," AGARD CP-494, Oct. 1990, pp. 21-1–21-15.

[5]Sarpkaya, T., "On Stationary and Travelling Vortex Break-

downs," *Journal of Fluid Mechanics*, Vol. 45, Pt. 3, Feb. 1971, pp. 545–559.

[6]Jumper, E. J., Nelson, R. C., and Cheung, K., "A Simple Criterion for Vortex Breakdown," AIAA Paper 93-0866, Jan. 1993.

[7]Leibovich, S., "The Structure of Vortex Breakdown," *Annual Review of Fluid Mechanics*, Vol. 10, 1978, pp. 221–246.

[8]Faler, J. H., and Leibovich, S., "Disrupted States of Vortex Flow and Vortex Breakdown," *Physics of Fluids*, Vol. 20, No. 9, 1977, pp. 1385–1400.

[9]Kegelman, J., and Roos, F., "Effects of Leading-Edge Shape and Vortex Burst on Flowfield of a 70 Degree Sweep Delta-Wing," AIAA Paper 89-0086, Jan. 1989.

[10]Gad-el-Hak, M., and Blackwelder, R. F., "The Discrete Vortices from a Delta Wing," *AIAA Journal*, Vol. 23, No. 6, 1985, pp. 961, 962.

[11]Huyer, S. A., "Forced Unsteady Separated Flows on a 45 Degree Delta Wing," Ph.D. Dissertation, Univ. of Colorado, Boulder, CO, May 1991, p. 73.

[12]Cornelius, K. C., "3-D Analysis of Laser Measurements of Vortex Bursting on a Chined Forebody Fighter Configuration," AIAA Paper 90-3020, Aug. 1990.

[13]Beyers, M. E., and Ericsson, L. E., "Ground Facility Interference in Aircraft Configurations with Separated Flow," *Journal of Aircraft*, Vol. 30, No. 5, 1993, pp. 682–688.

[14]Roos, F. W., and Kegelman, J. T., "An Experimental Investigation of Sweep-Angle Influence on Delta-Wing Flows," AIAA Paper 90-0383, Jan. 1990.

[15]McKernan, J. F., Payne, F. M., and Nelson, R. C., "Vortex Breakdown Measurements on a 70 Deg Sweepback Delta Wing," *Journal of Aircraft*, Vol. 25, No. 11, 1988, pp. 991, 992.

[16]Ericsson, L. E., "The Fluid Mechanics of Slender Wing Rock," *Journal of Aircraft*, Vol. 21, No. 5, 1984, pp. 322–328.

[17]Earnshaw, P. B., and Lawford, J. A., "Low-Speed Wind-Tunnel Experiments on a Series of Sharp-Edged Delta Wings," R&M 3424, Aeronautical Research Council, UK, March 1964.

[18]Wentz, W. H., and Kohlman, D. L., "Vortex Breakdown on Slender Sharp-Edged Wings," *Journal of Aircraft*, Vol. 8, No. 3, 1971, pp. 156–161.

[19]Payne, F. M., Ng, T. T., and Nelson, R. C., "Visualization and Wake Surveys of the Vortical Flow over a Delta Wing," *AIAA Journal*, Vol. 26, No. 2, 1988, pp. 137–143.

[20]Erickson, G. E., "Flow Studies of Slender Wing Vortices," AIAA Paper 80-1423, Jan. 1980.

[21]Lambourne, N. C., and Bryer, D. W., "The Bursting of Leading-Edge Vortices—Some Observations and Discussion of the Phenomenon," R&M 3282, Aeronautical Research Council, UK, April 1961.

[22]Ericsson, L. E., and King, H. H. C., "Effect of Cross-Sectional Geometry on Slender Wing Unsteady Aerodynamics," *Journal of Aircraft*, Vol. 30, No. 5, 1993, pp. 793–795.

[23]Erickson, G. E., "Water Tunnel Studies of Leading-Edge Vortices," *Journal of Aircraft*, Vol. 19, No. 6, 1982, pp. 442–448.

[24]Hanff, E. S., and Ericsson, L. E., "Multiple Roll Attractors of a Delta Wing at High Incidence," *AGARD Symposium on Vortex Flow Aerodynamics*, AGARD CP 494, Oct. 1990, pp. 31-1–31-10.

[25]Jenkins, J. E., and Myatt, J. H., "Body-Axis Rolling Motion Critical States of a 65-Degree Delta Wing," AIAA Paper 93-0621, Jan. 1993.

[26]Thompson, S. A., Arena, A. S., Jr., Nelson, R. C., and Batill, S. M., "Dynamic Surface Pressure Measurements on a Delta Wing Constrained to a Pitching or Rolling Motion," *Proceedings from High Angle of Attack Technology Conference*, NASA Langley Research Center, Hampton, VA, 1992, pp. 1003–1023 (NASA CP 3149).